Modeling the Control of Fixational Eye Movements with Neurophysiological Delays

Konstantin Mergenthaler[1,2,*] and Ralf Engbert[1,2,3]

[1]Helmholtz Center for Mind and Brain Dynamics, University of Potsdam, Potsdam, Germany
[2]Department of Psychology, University of Potsdam, Potsdam, Germany
[3]Center for Dynamics of Complex Systems, University of Potsdam, Potsdam, Germany

(Received 2 August 2006; published 29 March 2007)

We propose a model for the control of fixational eye movements using time-delayed random walks. Fixational eye movements produce random displacements of the retinal image to prevent perceptual fading. First, we demonstrate that a transition from persistent to antipersistent correlations occurs in data recorded from a visual fixation task. Second, we propose and investigate a delayed random-walk model and get, by comparison of the transition points, an estimate of the neurophysiological delay. Differences between horizontal and vertical components of eye movements are found which can be explained neurophysiologically. Finally, we compare our numerical results with analytic approximations.

DOI: 10.1103/PhysRevLett.98.138104 PACS numbers: 87.19.Dd, 87.19.St, 89.75.Da

Visual perception of stationary scenes requires accurate fixation on a target object. Paradoxically, our eyes perform miniature (or fixational) eye movements involuntarily during the act of fixation. Fixational eye movements (FEM) counteract perceptual fading, which occurs in response to artificially stabilized retinal input [1]. Recent evidence suggests that FEM both modulate and are influenced by diverse neural and behavioral processes ranging from oculomotor control [2,3], sensory bursting phenomena [4], and perceptual transitions [5] to visual attention [6]. Therefore, a mathematical model of FEM can potentially contribute specific predictions to various areas of cognitive neuroscience.

In this Letter, we first study the correlations in high-resolution time series of fixational eye movements recorded during exceptionally long fixation intervals. Correlations are estimated using measures of lagged standard deviations [7,8] as well as detrended fluctuation analysis (DFA) [8–10]. Second, we propose a model based on the concept of time-delayed random walks [11–16]. We show that the value of the time delay, which had to be chosen for best agreement between model simulations and experimental data, is highly compatible with our current knowledge of the neural organization of the oculomotor circuitry [17,18]. Finally, we compare our numerical results with analytical approximations.

In our experiment, we recorded the horizontal and vertical eye movements during a fixation task, using a high-speed video-based eye tracker with a sampling rate of $T_s = 500$ Hz (EyeLink-II, SR Research, Toronto, Canada) and an instrument spatial resolution $<0.01°$ visual angle. Participants (the two authors and 20 students of the University of Potsdam) were required to fixate a black square (3×3 pixels on a computer display or 7.2 arc min) on white background. Each participant performed 30 trials with a duration of 20 seconds, while an online check for eye blinks reduced loss of data. After preprocessing, we obtained 622 valid trials. The horizontal component of a typical trajectory of fixational eye movements is shown in Fig. 1. FEM consist of three different kinematic components, i.e., drift, tremor, and microsaccades [4]. Drift is generally believed to represent oculomotor noise. Tremor is a very small-amplitude ($< 0.01°$) oscillatory component not resolved in video-based eye tracking devices and is therefore neglected here. Microsaccades represent ballistic small-amplitude movements embedded in the drift component [3,6].

A fundamental problem of random walks is related to the estimation of short and long range correlations [19]. The FEM data show statistical properties similar to the trajectory of the center of gravity during quiet standing [20,21]. An analysis of the scaling behavior [2,6,8,9,20] is a basis for model building. As in earlier work [6,9], standard deviation analysis (SDA) [7,8] and detrended fluctuation analysis (DFA) [9,10] reveal two different types of scaling behavior on short and long time scale [Fig. 2(a) and 2(b)].

The SDA [8] is a measure of the lagged standard deviation and is computed by

$$D^2(l) = \frac{1}{2(N-l)} \sum_{i=0}^{N-l} [x(i-l) - x(i) - \bar{x}(l)]^2, \quad (1)$$

where $x(i)$ denotes the ith data point of the horizontal

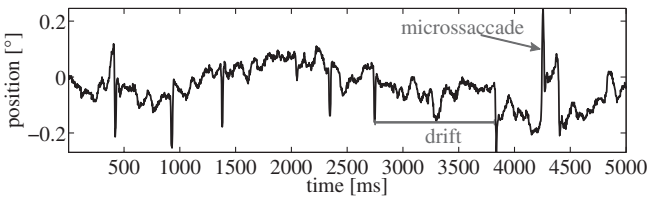

FIG. 1. First five seconds of the horizontal component of the eye trajectory during fixational eye movements. Microsaccades are ballistic small-amplitude movements embedded in slower movements.

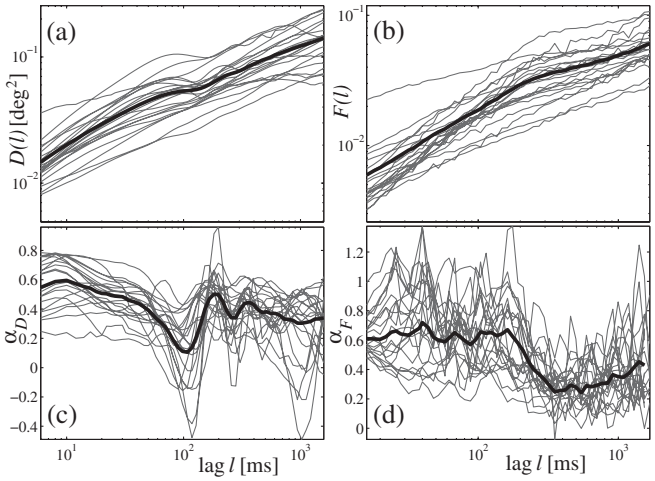

FIG. 2. The scaling analyses for the data. (a) The scaling behavior of the SDA. (b) Output of the DFA shows two scale behavior. (c) The slope of the SDA shows a prominent trough at $l = 100$ ms. (d) Slope of the DFA. The gray lines denote the means of each participant, the black line the mean over all participants.

position signal. The mean value for the distance is denoted by $\bar{x}(l) = 1/N \sum_i^N x(i - l) - x(i)$. To investigate power-law behavior of the form $D^2(l) \propto l^{2\alpha}$, we analyze log-log plots of $D(l)$ in [deg^2] versus l in [ms] [Fig. 2(a)] and the slope of $D(l)$ [Fig. 2(c)]. The local slope is computed by fitting a linear function to five consecutive points (running average). Thus, the local α can directly be read off from the plot in Fig. 2(c). For $\alpha = 0.5$ we have an uncorrelated signal, while for $\alpha < 0.5$ the signal is antipersistent and for $\alpha > 0.5$ it is persistent. We find a transition between these two regimes, which is indicated in the SDA by the sharp trough at $l = 100$ ms [Fig. 2(c)].

For the DFA [8–10] we compute a velocity time series from the eye-position data by $v(i) = T_s(x(i + 1) - x(i))$. The detrended fluctuation analysis (DFA-p) is capable of investigating scaling behavior in nonstationary data while removing polynomial trends of order $p - 1$. It consists of five steps: (a) performing a cumulative sum of the investigated data, (b) cutting the data of length L in $N_l = \lfloor L/l \rfloor$ segments ν of length l where $2p + 1 \leq l \leq L/10$, (c) fitting of the best polynomial trend y_ν of order p on the data in each segment, (d) computing the mean of the mean squared deviation of the data adjusted by the trend, i.e.,

$$F^2(l) = \frac{1}{N_l} \sum_{\nu=1}^{N_l} \frac{1}{l} \sum_{i=1}^{l} [v((\nu - 1)l + i) - y_\nu]^2, \qquad (2)$$

and (e) determining the exponent from log-log plots of $F(l)$ versus l [Fig. 2(b)] analogously to the SDA above.

Applying the DFA-2 to the horizontal eye-movement data demonstrates persistent behavior on the short time scale and antipersistent behavior on the long time scale (Fig. 2) with a clear transition between the two regimes [2,22]. This dynamical behavior is physiologically functional. First, persistent behavior on the short time scale enhances retinal image slip, which is needed to counteract retinal adaptation in response to constant input. Second, the antipersistent behavior on the long time scale stabilizes the current fixation. As noted in [23], the estimation of the numerical value of the lag at the transition point is generally overestimated by the DFA. Therefore, we use the SDA for the estimation of the transition point. Removing of all microsaccades (as in [2]) and performing the same analyses shows that the results for the correlations are not specifically due to microsaccades.

Motivated by the delayed random-walk models for postural sway proposed by Ohira and Milton [13] and Yao, Yu, and Essex [12] and the assumption that the antipersistent behavior for the long time scale arises from a neural control mechanism, we formulated a delayed random-walk model for FEM. A basic problem is whether movements are controlled on the level of eye position or eye velocity. For our model we can exploit the fact that the activity of oculomotor neurons [17,18] is given as the sum of excitatory burst neurons (EBN) and tonic units (TU). The firing rate of the EBN is related to active movements independent of eye position; therefore, EBN activity determines eye velocity. The activity of TU is proportional to the fixation position relative to the center of the visual field (eccentricity), i.e., TU serve a function in gaze holding. During FEM, however, changes in absolute eye position are negligible (i.e., less than 1°). As a consequence, we do not expect systematic variations in TU activity. In our model, TU activity can be approximated by an additional noise source added to eye position.

We implement our model as a discrete map. First, we use an autoregressive term for the EBN activity $w_{i+1} = (1 - \gamma)w_i$ to generate the persistent correlations at the short time scale, created by the eye's inertia. The second term, a noise term ξ_i, represents EBN baseline activity where ξ_i are uncorrelated Gaussian random numbers with $\langle \xi_i \rangle = 0$ and $\langle \xi_i \xi_j \rangle = \sigma^2 \delta_{ij}$ and σ is the standard deviation of the noise. A third term introduces negative feedback (with a delay) in order to stabilize FEM and to generate antipersistent behavior on the long time scale, $-\lambda \tanh(\epsilon w_{i-\tau})$ [12]. The parameters are the physiological delay, τ, the feedback strength, λ, and a parameter for variation of the steepness of the control function, ϵ.

The influence of the EBN is added to the TU activity, an additive noise term η_i with $\langle \eta_i \rangle = 0$ and $\langle \eta_i \eta_j \rangle = \rho^2 \delta_{ij}$, where ρ is the standard deviation. Taken together, we can write our model as

$$\begin{aligned} w_{i+1} &= (1 - \gamma)w_i + \xi_i - \lambda \tanh(\epsilon w_{i-\tau}), \\ x_{i+1} &= x_i + w_{i+1} + \eta_i. \end{aligned} \qquad (3)$$

In this model, all eye positions x_i are stable because of the lack of a systematic variation of TU activity with eccentricity (see above). Moreover, it important to note that all

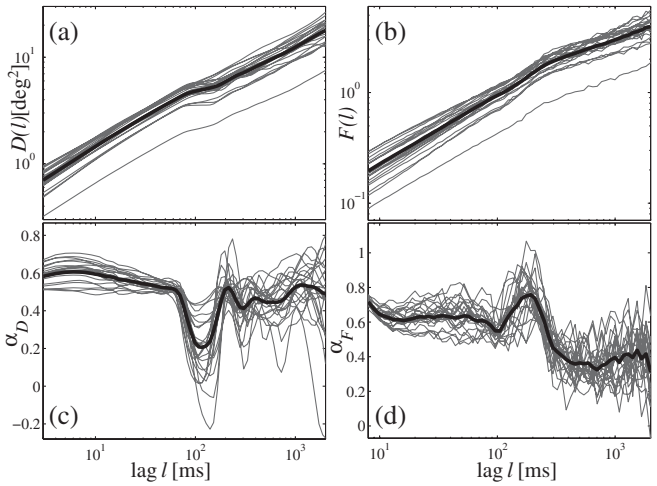

FIG. 3. The scaling analyses for the model with $\gamma = 0.25$, $\lambda = 0.15$, $\sigma = 0.075$, $\rho = 0.35$ $\epsilon = 1.1$, and $\tau = 70$. To mimic individual variations we added normal distributed parameter variations with a standard deviation of 0.1 for ρ and ϵ and standard deviation of 0.02 for σ, γ, and λ and introduced deviations for τ drawn from a binomial distribution with $p = 0.5$ and $N = 20$. (a) Scaling behavior estimated via SDA. (b) Results from DFA. (c) Slope of the SDA plot. (d) Slope analysis for DFA.

parameters of our model have direct physiological interpretations.

Systems with delayed negative feedback typically produce oscillatory behavior [11,12,14,16]. Here, we consider the case of low gain, where oscillations are not dominant (but see [24]). Different from postural sway data, we did not find a third time scale, where the scaling exponent tends to zero. Such a time scale with slope of zero is related to the high-gain regime, which we do not consider here.

For numerical simulations, we simulated 200 000 iterates, where one iteration step corresponds to 1 ms, and analyzed the last 20 000 data points only, to exclude potential transient effects. The DFA for the model is based on the velocity time series generated from the position x_i of Eq. (3) as described for the eye-position data. A parameter set that is appropriate to reproduce the scaling behavior of the FEM data is $\gamma = 0.25$, $\lambda = 0.15$, $\sigma = 0.075$, $\rho = 0.35$, and $\epsilon = 1.1$. For the horizontal component of the FEM a time delay of $\tau_{\text{hor.}} = 70$ ms leads to optimal correspondence between experimental data and model simulations (Fig. 3). This result is in good agreement with our current knowledge of the oculomotor circuitry [17,18]: visual information entering the retina needs $t_p = 40$ ms to reach the superior colliculus (SC) [25], the top-level control structure for saccadic eye movements in the brain stem. Furthermore, stimulation of cells in the SC generates an eye movement only $t_m = 20$ ms later [26]. Therefore, a lower bound for the (visually guided or external) control loop is $\tau_{\text{hor.}} = 60$ ms. Additionally, we investigated the vertical component of the eyes (not shown) by using the same techniques. Interestingly, we obtained a smaller delay of $\tau_{\text{vert.}} = 40$ ms for vertical FEM, if all other parameters are fixed. This smaller numerical value is highly compatible with the existence of an internal (i.e., not visual) physiological control loop for vertical saccades [17] and suggests independence between vertical and horizontal FEM components.

Next, we present analytical approximations for the correlations on the two time scales. For the short time scale we estimate the scaling behavior from the slope of the graph between lags 1 and 2, i.e.,

$$2H_s = \frac{\log\frac{D^2(2)}{D^2(1)}}{\log(2)} \quad \text{with } D^2(N) = \langle (x_{k+N} - x_k)^2 \rangle. \tag{4}$$

Because measurement noise η_i and velocities w_{i+1} are statistically independent, we obtain $D^2(1) = \langle (w_{k+1} + \eta_k)^2 \rangle = \langle w^2 \rangle + \rho^2$. We assume stationarity and set $\gamma' = 1 - \gamma$, i.e., $\langle w_{k+1}^2 \rangle = \gamma'^2 \langle w_k^2 \rangle + \sigma^2 + \lambda^2 \langle \tanh^2(\epsilon w_{k-\tau}) \rangle - 2\lambda\gamma' \langle w_k \tanh(\epsilon w_{k-\tau}) \rangle$. We approximate $\tanh(\epsilon w_{k-\tau}) \approx \epsilon w_{k-\tau}$. Numerically, we observe a strongly negative autocorrelation function at lag τ. Therefore, we set $\langle w_k \tanh(\epsilon w_{k-\tau}) \rangle \approx -\epsilon \langle w_k^2 \rangle$. Thus, we obtain the equation

$$\langle w^2 \rangle = \frac{\sigma^2}{1 - \gamma'^2 - \lambda^2\epsilon^2 - 2\lambda\epsilon\gamma'}. \tag{5}$$

For $D^2(2)$ we iterate Eq. (3),

$$D^2(2) = \langle (1 - \gamma' w_{k+1} + \xi_{k+1} - \lambda \tanh(\epsilon w_{k+1-\tau}) + \eta_k + \eta_{k+1})^2 \rangle.$$

We use the approximation for the tanh function again and obtain $D^2(2) = (1 - \gamma' + \lambda^2)\langle w^2 \rangle + 2\rho^2 + \sigma^2$. Taken together for the short time scale our approximation yields the formula

$$H_s = \frac{1}{2\log 2} \log\left(\frac{(1 - \gamma'^2 + \lambda^2)\langle w^2 \rangle + 2\rho^2 + \sigma^2}{\langle w^2 \rangle + \rho^2} \right), \tag{6}$$

where $\langle w^2 \rangle$ is obtained from Eq. (5).

For the long time scale, we have to account for effects of the delay term. Thus, we calculate the slope between lags τ and 2τ, i.e.,

$$2H_l = \frac{1}{\log(2\tau/\tau)} \log\frac{D^2(2\tau)}{D^2(\tau)}. \tag{7}$$

Generally, iteration of Eq. (3) gives

$$D^2(N) = \left\langle \left(\sum_{j=1}^{N} \gamma' w_{k+j} + \xi_{k+j} - \lambda \tanh(\epsilon w_{k+j-\tau}) + \eta_{k+j} \right)^2 \right\rangle.$$

Here we assume that the major contributions to $D^2(N)$ arise from terms with differences of $l = 0$, 1, $\tau - 1$, τ, $\tau + 1$. With $\langle w_{k+1} w_k \rangle = \gamma' \langle w^2 \rangle$ and again the approximation for tanh function we can write the mean square displacements as $D^2(\tau) = \tau\Delta$ and $D^2(2\tau) = 2\tau\Delta - \tau\Lambda$ with $\Delta = \rho^2 + (2\gamma'^2 + 1)\sigma^2 + (\gamma'^2 + \lambda^2\epsilon^2 + 2\gamma'^3 + 2\lambda^2\gamma')\langle w^2 \rangle$ and $\Lambda = (4\lambda\gamma' + 2\lambda)\sigma^2 + (4\lambda\gamma'^2 + 2\lambda\gamma')\langle w^2 \rangle$. Using these

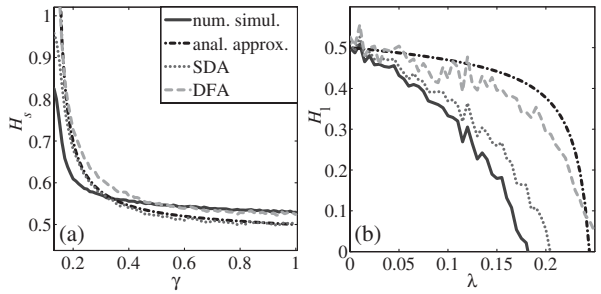

FIG. 4. Comparison of analytical approximation (dash-dotted line) with numerical values (solid line), SDA (dotted line), and DFA (dashed line). (a) Short time scale: H_s analytically by Eq. (6), numerically by Eq. (4), SDA for $l = 1$ to 20 and DFA for $l = 6$ to 100. (b) Long time scale: H_l analytically by Eq. (8), numerically by Eq. (7), SDA for $l = 70$ to 210 and DFA for $l = 400$ to 2000.

abbreviations, we can write the approximation for the long time scale as

$$H_l = \frac{1}{2\log 2} \log\left(\frac{2t\Delta - \tau\Lambda}{\tau\Delta}\right). \quad (8)$$

To check the validity of our analytical calculations, we compare the results with numerical simulations. In Fig. 4(a) we show the comparison of values of H_s for the short time scale as a function of γ. Around the chosen value $\gamma = 0.25$ the analytical approximation is in good agreement with the numerical simulation. For the long time scale we plot the dependence of H_l on λ [Fig. 4(b)]. Qualitatively, analytical approximation and numerical results agree; however, the analytical results are closer to the results obtained via DFA. Thus, the analytical calculations confirm the parameter dependence of the scaling exponents observed in the numerical simulations.

In summary, we replicated our previous results on a transition from persistent to antipersistent behavior in fixational eye movements [2,9] for extraordinarily long fixation intervals with a duration of 20 s. As a starting point for mathematical modeling, we investigated the transition point between the two dynamical regimes and found a pronounced trough in the SDA at the critical value for the time lag. We introduced a nonlinear, delayed negative feedback, which generated antipersistent behavior on the long time scale in a low-gain regime. Our results were checked with analytical calculations for the scaling exponents. Time-delayed control is a neurophysiologically highly plausible feature of the brain stem oculomotor circuitry [17]. More specifically, our model could explain the differences between the control of horizontal and vertical eye movements.

We thank Shay Moshel, John G. Milton, André Longtin, and Reinhold Kliegl for valuable discussions. This work was supported by Deutsche Forschungsgemeinschaft (Grant No. KL 955/3) and by MWFK Brandenburg.

*Electronic address: Konstantin.Mergenthaler@uni-potsdam.de

[1] R. W. Ditchburn and B. Ginsborg, Nature (London) **170**, 36 (1952); L. A. Riggs, F. Ratliff, J. C. Cornsweet, and T. N. Cornsweet, J. Opt. Soc. Am. **43**, 495 (1953); for an overview, see R. M. Pritchard, Sci. Am. **204**, 72 (1961).
[2] R. Engbert and R. Kliegl, Psychol. Sci. **15**, 431 (2004).
[3] R. Engbert and K. Mergenthaler, Proc. Natl. Acad. Sci. U.S.A. **103**, 7192 (2006).
[4] S. Martinez-Conde, S. L. Macknik, and D. H. Hubel, Nat. Neurosci. **3**, 251 (2000); Proc. Natl. Acad. Sci. U.S.A. **99**, 13 920 (2002); for an overview, see Nat. Rev. Neurosci. **5**, 229 (2004).
[5] S. Martinez-Conde, S. L. Macknik, X. G. Troncoso, and T. A. Dyar, Neuron **49**, 297 (2006); see also R. Engbert, Neuron **49**, 168 (2006).
[6] R. Engbert and R. Kliegl, Vision Res. **43**, 1035 (2003); R. Engbert, Prog. Brain Res. **154**, 177 (2006).
[7] J. J. Collins and C. J. De Luca, Exp. Brain Res. **95**, 308 (1993).
[8] N. Scafetta and P. Grigolini, Phys. Rev. E **66**, 036130 (2002).
[9] J.-R. Liang, S. Moshel, A. Zivotofsky, A. Caspi, R. Engbert, R. Kliegl, and S. Havlin, Phys. Rev. E **71**, 031909 (2005).
[10] C.-K. Peng, S. Buldyrev, S. Havlin, M. Simons, H. Stanley, and A. Goldberger, Phys. Rev. E **49**, 1685 (1994).
[11] T. Ohira and T. Yamane, Phys. Rev. E **61**, 1247 (2000).
[12] W. Yao, P. Yu, and C. Essex, Phys. Rev. E **63**, 021902 (2001).
[13] T. Ohira and J. G. Milton, Phys. Rev. E **52**, 3277 (1995).
[14] T. Ohira, Phys. Rev. E **55**, R1255 (1997).
[15] C. W. Eurich and J. G. Milton, Phys. Rev. E **54**, 6681 (1996).
[16] A. Longtin, J. G. Milton, J. E. Bos, and M. C. Mackey, Phys. Rev. A **41**, 6992 (1990).
[17] A. K. Moschovakis, C. A. Scudder, and S. M. Highstein, Prog. Neurobiol. **50**, 133 (1996).
[18] D. L. Sparks, Nat. Rev. Neurosci. **3**, 952 (2002).
[19] R. Metzler and J. Klafter, Phys. Rep. **339**, 1 (2000).
[20] J. J. Collins and C. J. De Luca, Phys. Rev. Lett. **73**, 764 (1994).
[21] M. Rosenblum, G. Fisov, R. Kuuz, and B. Pompe, in *Nonlinear Analysis of Physiological Data*, edited by H. Kantz, J. Kurths, and G. Mayer-Kress (Springer, New York, 1998), p. 283.
[22] L. S. Liebovitch and W. Yang, Phys. Rev. E **56**, 4557 (1997).
[23] J. W. Kantelhardt, E. Koscielny-Bunde, H. H. A. Rego, S. Havlin, and A. Bunde, Physica (Amsterdam) **295A**, 441 (2001).
[24] Different from the case of FEM studied here, there might be a high-gain regime in the oculomotor (saccadic) system [see: [15] and L. Moreau and E. Sontag, Phys. Rev. E **68**, 020901 (2003)]. We investigated the transition to such a regime numerically. If all other parameters are fixed, we observed a bifurcation at $\epsilon \approx 1.6$.
[25] D. Guitton, in *Eye Movements*, edited by R. H. S. Carpenter (MacMillan, London, 1992), p. 244.
[26] D. L. Sparks, Physiol. Rev. **66**, 118 (1986).